REPORT DOCUMENTATION PAGE

Form Approved
OMB No. 074-0188

1. AGENCY USE ONLY (Leave blank)

2. REPORT DATE
October 31, 1995

3. REPORT TYPE AND DATES COVERED
Technical report, 1995

4. TITLE AND SUBTITLE
Theoretical Topics in Wave Propagation in a Random Medium

5. FUNDING NUMBERS
N/A

6. AUTHOR(S)
George Lamb

7. PERFORMING ORGANIZATION NAME(S) AND ADDRESS(ES)

Mathematics Department
The University of Arizona
Tucson, AZ 85721

8. PERFORMING ORGANIZATION REPORT NUMBER
N/A

9. SPONSORING / MONITORING AGENCY NAME(S) AND ADDRESS(ES)
SERDP
901 North Stuart St. Suite 303
Arlington, VA 22203

10. SPONSORING / MONITORING AGENCY REPORT NUMBER
N/A

11. SUPPLEMENTARY NOTES

12a. DISTRIBUTION / AVAILABILITY STATEMENT
Approved for public release: distribution is unlimited

12b. DISTRIBUTION CODE
A

13. ABSTRACT *(Maximum 200 Words)*
Three aspects of wave propagation in a random medium are considered. The first is the scattering of a plane compressional wave by a spherical inhomogeneity of specified radius. This result is then averaged over a Rayleigh distribution of sphere radii. As a second topic, the scattering by a medium in which an elastic parameter varies randomly is considered. When the randomness is assumed to be described by a Gaussian correlation function, it is found that the frequency and angular dependence of the scattering is the same as that obtained in the previous calculation with the Rayleigh distribution when the average diameter of the spheres is set equal to the correlation distance appearing in the random medium.

The third topic considered is the effect of the randomness on the focusing of the wave. The total incident sound field may be viewed as being composed of a sum of coherent field reflected from an object of interest and an incoherent field resulting from the scattering due to inhomogeneities in the surrounding medium. The fluctuations in the imaging of the incoherent field can be decreased by increasing the size of the receiving system and this dependence on receiver size will have been achieved when the receiver has been increased to a size equal to about twice the correlation length of the fluctuations in the incident field.

14. SUBJECT TERMS
wave propagation, plane compressional wave, spherical inhomogeneity, Rayleigh distribution, SERDP

15. NUMBER OF PAGES
24

16. PRICE CODE
N/A

17. SECURITY CLASSIFICATION OF REPORT	18. SECURITY CLASSIFICATION OF THIS PAGE	19. SECURITY CLASSIFICATION OF ABSTRACT	20. LIMITATION OF ABSTRACT
unclass	unclass	unclass	UL

NSN 7540-01-280-5500

Standard Form 298 (Rev. 2-89)
Prescribed by ANSI Std. Z39-18
298-102

October 31, 1995

Theoretical Topics in Wave Propagation in a Random Medium

George Lamb
Mathematics Department, The University of Arizona, Tucson, AZ 85721

Abstract

Three aspects of wave propagation in a random medium are considered. The first is the scattering of a plane compressional wave by a spherical inhomogeneity of specified radius. This result is then averaged over a Rayleigh distribution of sphere radii. As a second topic, the scattering by a medium in which an elastic parameter varies randomly is considered. When the randomness is assumed to be described by a Gaussian correlation function, it is found that the frequency and angular dependence of the scattering is the same as that obtained in the previous calculation with the Rayleigh distribution when the average diameter of the spheres is set equal to the correlation distance appearing in the random medium.

The third topic considered is the effect of the randomness on the focusing of the wave. The total incident sound field may be viewed as being composed of a sum of a coherent field reflected from an object of interest and an incoherent field resulting from the scattering due to inhomogeneities in the surrounding medium. The fluctuations in the imaging of the incoherent field can be decreased by increasing the size of the receiving system and this dependence on receiver size is determined for a square receiver. It is found that most of the advantage to increasing receiver size will have been achieved when the receiver has been increased to a size equal to about twice the correlation length of the fluctuations in the incident field.

A. SCATTERING BY A SPHERICAL INHOMOGENEITY WITH AVERAGING OVER A RAYLEIGH DISTRIBUTION OF SCATTERING RADII

The sound pressure field scattered by a spherical inhomogeneity in a solid medium is examined. The wave motion is described by a standard theoretical model used in geophysical prospecting(1) in which shear waves are ignored. As is well known, the angular distribution of a scattered field is sharply peaked when the circumference of the scatterer is greater than the

wavelength of the incident wave. When the average scattering produced by an assemblage of scatterers of different radii is considered, however, the variation in the average field can be expected to be smoothed out. For wavelengths larger than or comparable to the circumference, there is little angular dependence and hence little effect due to averaging. The averaging is performed here with respect to a Rayleigh distribution. In the second part of this report it is shown that the average intensity scattered by a random medium with a Gaussian correlation function has the same dependence on frequency and scattering angle as that obtained for the spherical scatterers when the correlation length is set equal to the rms diameter of the spheres.

A.1 *The Theoretical Model*

As noted above, we use a simple model in which shear waves are ignored and only compressional waves are considered. The governing equations are taken to be

$$\rho \frac{\partial^2 \xi}{\partial t^2} = -\nabla P \qquad\qquad (1)$$
$$P = -B \nabla \bullet \xi$$

where $P(\mathbf{r},t)$ and $\xi(\mathbf{r},t)$ are the sound pressure and elastic displacement in the medium, respectively. The parameter ρ is the density of the medium and in order to keep the analytical model as simple as possible, is assumed to be a constant. The bulk modulus B is written in the form $B = B_0 - \delta B$ where B_0 is the constant background modulus and the scattering inhomogeneity is taken to be

$$\delta B = \begin{cases} \delta B_0 & , \quad r < a \\ 0 & , \quad r > a \end{cases} \qquad\qquad (2)$$

where δB_0 is a constant.

The wave equation that now follows from Eq.(1) has the form[2]

$$\nabla^2 P - \frac{\rho}{B} \frac{\partial^2 P}{\partial t^2} = 0 \qquad\qquad (3)$$

Confining attention to a wave at a single frequency ω by writing $P(\mathbf{r},t) = p(\mathbf{r})e^{-i\omega t}$, we find that

Eq.(3) has the form

$$\nabla^2 p + \left(\tfrac{\omega}{c_0}\right)^2 p = -\left(\tfrac{\omega}{c_0}\right)^2 \frac{\delta B_0}{B_0} p \tag{4}$$

where $c_0^2 = B_0/\rho_0$.

The scattered field due to an incident plane wave $p_{inc.} = p_0 e^{i\mathbf{k}\cdot\mathbf{r}}$ is given by

$$p_{sc} = p - p_{inc.} = k^2 \frac{\delta B_0}{B_0} \int_V d^3\mathbf{r}' \frac{e^{ik|\mathbf{r}-\mathbf{r}'|}}{4\pi|\mathbf{r}-\mathbf{r}'|} p(\mathbf{r}') \tag{5}$$

where the integration is performed over the spherical volume of the scatterer. At distances that are a number of wavelengths away from the scattering volume, the expression for the scattered field reduces to

$$p_{sc} = \frac{k^2}{4\pi} \frac{\delta B_0}{B_0} \frac{e^{ikr}}{r} \int_V d^3\mathbf{r}' e^{-i\mathbf{k}_s\cdot\mathbf{r}'} p(\mathbf{r}') \tag{6}$$

where $\mathbf{k}_s$ is in the direction in which the scattering is observed and has a magnitude equal to $k = \omega/c_0$. For weak inhomogenieties, one may expect the field within the scatterer to be nearly equal to the incident field and thus set $p(\mathbf{r}') = p_{inc.} = p_0 e^{i\mathbf{k}\cdot\mathbf{r}'}$ in the integrand of Eq.(6). The scattered field is then

$$\frac{p_{sc}}{p_0} = \frac{k^2}{4\pi} \frac{\delta B_0}{B_0} \frac{e^{ikr}}{r} \int_V d^3\mathbf{r}' e^{-i\mathbf{K}\cdot\mathbf{r}'} \tag{7}$$

where $\mathbf{K} = \mathbf{k}_s - \mathbf{k}$. The integral is now readily evaluated and yields

$$\frac{p_{sc}}{p_0} = k^2 \frac{\delta B_0}{B_0} \frac{e^{ikr}}{r} \left[a^3 \frac{j_1(Ka)}{Ka} \right] \tag{8}$$

where $j_1(x)$ is a spherical Bessel function given by $j_1(x) = \sin x/x^2 - \cos x/x$ and $K = 2k\sin(\theta/2)$ in which θ is the scattering angle, i.e., the angle between $\mathbf{k}_s$ and $\mathbf{k}$. Polar plots of this result for various values of ka are shown in Fig. 1. As expected, side lobes in the scattered

field do not appear until $ka = 2\pi/\lambda$ becomes greater than unity. Since interest in the present project is confined to low frequencies, plots of higher ka values have not been considered.

A.2 *Averaging over a Rayleigh distribution of scattering radii*

As seen from Fig. 1, the angular dependence of the scattered wave becomes quite pronounced when $ka > 1$. The net effect of the scattering due to an assemblage of scatterers of different sizes should be a smearing out of these sharp peaks. When the radii are assumed to vary according to a Rayleigh distribution, defined by

$$f_R(a) \equiv \frac{a}{a_0^2} e^{-a^2/2a_0^2} \tag{9}$$

where a_0 is the rms size of the scatterers, we obtain the average of the scattered field given in Eq.(8) in the form

$$\begin{aligned} \left\langle \frac{p_{sc}}{p_0} \right\rangle_{\text{Rayl.}} &= \int_0^\infty da \frac{a}{a_0^2} e^{-a^2/2a_0^2} \left[\frac{p_{sc}(a)}{p_0} \right] \\ &= k^2 \frac{\delta B_0}{B_0} \frac{e^{ikr}}{r} I \end{aligned} \tag{10}$$

where

$$I \equiv \frac{1}{Ka_0^2} \int_0^\infty da e^{-a^2/2a_0^2} a^3 j_1(Ka) \tag{11}$$

When j_1 is written in terms of an ordinary cylindrical Bessel function as $j_1(x) = (\pi/2x)^{1/2} J_{3/2}(x)$, the integral in Eq.(11) takes on a standard tabulated form[3] and yields the much smoother distribution

$$\left\langle \frac{p_{sc}}{p_0} \right\rangle_{\text{Rayl.}} = \sqrt{\frac{\pi}{2}} \frac{\delta B_0}{B_0} \frac{e^{ikr}}{kr} (ka_0)^3 e^{-2[ka_0 \sin(\theta/2)]^2} \tag{12}$$

which is shown in Fig. 2. Since $0 < \theta < \pi$, no sidelobes are generated by the term $\sin(\theta/2)$ in this result. For $ka < 1$, the averaging is seen to produce little effect while for larger ka values the peaks are smoothed out.

Note that the squared magnitude of the scattered field is given by

$$\left|\left\langle \frac{p_{sc}}{p_0} \right\rangle_{\text{Rayl.}}\right|^2 = \frac{\pi}{2}\left(\frac{\delta B_0}{B_0}\right)^2 \frac{1}{(kr)^2}(ka_0)^6 e^{-4[ka_0 \sin(\theta/2)]^2} \tag{13}$$

In the next section it will be shown that this same dependence on wave number k and scattering angle θ is obtained for the scattering by a random medium when the randomness is described by a Gaussian correlation function.

B. SCATTERING BY RANDOM FLUCTUATIONS IN THE BULK MODULUS

We now consider the scattering per unit volume due to random fluctuations in the bulk modulus of the medium. Returning to Eq. (4) and replacing $\delta B_0/B_0$ by a randomly varying function $f(\mathbf{r})$, Eq. (5) is replaced by

$$p_{sc} = k^2 \int_V d^3\mathbf{r}' f(\mathbf{r}') \frac{e^{ik|\mathbf{r}-\mathbf{r}'|}}{4\pi|\mathbf{r}-\mathbf{r}'|} p(\mathbf{r}') \tag{1}$$

where the integration is now over the entire random medium. Again using the far field assumption $r \gg r'$, we have

$$\frac{p_{sc}}{p_0} = \frac{k^2}{4\pi}\frac{e^{ikr}}{r}\int_V d^3\mathbf{r}' f(\mathbf{r}') e^{-i\mathbf{K}\cdot\mathbf{r}'} \tag{2}$$

The scattered energy is proportional to $p_{sc}(\mathbf{r})^* p_{sc}(\mathbf{r}) = |p_{sc}(\mathbf{r})|^2$. We now treat the scattered wave as a random variable and form a statistical average that is proportional to the scattered energy by considering

$$\frac{\langle |p_{sc}|^2 \rangle}{p_0^2} = \left(\frac{k^2}{4\pi}\right)^2 \frac{1}{r^2}\int_V d^3\mathbf{r}' \int_V d^3\mathbf{r}'' e^{i\mathbf{K}\cdot(\mathbf{r}'-\mathbf{r}'')} \langle f^*(\mathbf{r}') f(\mathbf{r}'') \rangle \tag{3}$$

Setting $\langle f^*(\mathbf{r}') f(\mathbf{r}'') \rangle = \mu(|\mathbf{r}' - \mathbf{r}''|)$, i. e., assuming that the correlation of fluctuations in the random variation is isotropic and homogeneous, we can introduce the coordinates $\mathbf{R} = (\mathbf{r}' + \mathbf{r}'')/2$ and $\boldsymbol{\rho} = (\mathbf{r}' - \mathbf{r}'')$ to obtain

$$\frac{\left\langle |p_{sc}|^2 \right\rangle}{p_0^2} = \left(\frac{k^2}{4\pi}\right)^2 \frac{1}{r^2} V \int_V d^3\boldsymbol{\rho} e^{i\mathbf{K}\cdot\boldsymbol{\rho}} \mu(|\boldsymbol{\rho}|) \tag{4}$$

where V is the total volume of the scattering region. Carrying out the integration over angles, we obtain the scattering per unit volume in the form

$$\frac{\left\langle |p_{sc}|^2 \right\rangle}{Vp_0^2} = \left(\frac{k^2}{4\pi}\right)^2 \frac{4\pi}{r^2 K} \int_0^\infty \rho d\rho \mu(\rho) \sin K\rho \tag{5}$$

The remaining integral may now be evaluated for various assumed forms for the correlation function $\mu(\rho)$. For the Gaussian form $\mu_G(\rho) = \mu_0 \exp(-\rho^2/L^2)$, we find[4]

$$\frac{\left\langle |p_{sc}|^2 \right\rangle_G}{Vp_0^2} = \frac{\mu_0}{16\sqrt{\pi} L^3} \frac{1}{(kr)^2} (kL)^6 e^{-[kL\sin(\theta/2)]^2} \tag{6}$$

This result is seen to have the same wave number and angular dependence as that obtained for the square of the Rayleigh distribution of spherical scatterers, and given in Eq.(13) of the previous section, when we set $L = 2a_0$, i.e., set the correlation length equal to the rms diameter of the spherical scatterers.

To give some indication of the sensitivity of these results to the assumed form of the correlation function, we summarize the results for the scattering distributions obtained from the correlation functions $\mu_E(\rho) = \mu_0 \exp(-\rho/L)$ and $\mu_S(\rho) = \mu_0 \mathrm{sech}\,(\rho/L)$. Graphs of these expressions are shown in Fig. 3. The corresponding scattering distributions are found to be[5]

$$\begin{aligned} \frac{\left\langle |p_{sc}|^2 \right\rangle_E}{Vp_0^2} &= \frac{\mu_0}{2\pi L^3} \frac{1}{(kr)^2} (kL)^6 \frac{1}{\left[(KL)^2 + 1\right]^2} \\ \frac{\left\langle |p_{sc}|^2 \right\rangle_S}{Vp_0^2} &= \frac{\mu_0 \pi^2}{32 L^3} \frac{1}{(kr)^2} (KL)^6 \frac{\sinh(\frac{\pi}{2} KL)}{\frac{\pi}{2} KL} \mathrm{sech}^2(\tfrac{\pi}{2KL}) \end{aligned} \tag{7}$$

Graphs of the KL dependence of these expressions, as well as that for the Gaussian, i.e., $f_G(k) = \exp[-(KL/2)]^2$, $f_E(k) = [(KL)^2 + 1]^{-2}$ and $f_S(k) = \mathrm{sech}^2\,(\pi KL/2)\,\sinh\,(\pi KL/2)/(\pi KL/2)$, are shown in Fig. 4. As expected, the sharper cutoff for the Gaussian $\mu_G(\rho)$ is reflected in a wider

spectrum for the transform $f_G(k)$. The negligible difference between the curves for f_E and f_S is of some interest in its own right since it shows that, at least in the present analysis, the much maligned cusp at the origin displayed by the exponential correlation function has little effect on the results.

The procedure adopted here, of assuming a form for the correlation function and then calculating the scattered field, is analogous to that of assuming a form for a refractive index or a scattering potential in deterministic scattering. The reverse procedure, i.e., that of using the scattering data to determine the form of the refractive index or potential (or correlation function) that gives rise to the scattering, is referred to as an inverse scattering problem and is a much more difficult consideration. For problems in deterministic scattering, it is now known that to be successful in such an endeavor one must know much more about the scattering data than is usually available. In particular, one must know either the angular distribution of the scattering at *all* angles at some one frequency or know the scattering at some one angle at *all* frequencies. It is usually impracticle to obtain such information. In addition, the exact form of the refractive index or scattering potential may depend critically on the scattering data, i.e., significant changes in the predicted form of the refractive index, potential or correlation function may result from small changes in the scattering data. Finally since the data collected may be expected to contain experimental error, it is usually impossible to determine any "correct" source of the scattering. Fortunately, scattering by random inhomogeneities is usually not extremely sensitive to the form of the correlation function and so a choice of convenience, frequently the Gaussian, is usually made.

C. THE INFLUENCE OF FLUCTUATIONS ON THE DIFFRACTION IMAGE OF A FOCUSING SYSTEM

The sound field incident upon the focusing system consists of a coherent part due to scattering by the object of interest and an incoherent part due to scattering by inhomogeneities in the medium. When the amplitude of the incoherent field becomes comparable to that of the coherent field, the image can be assumed to be no longer detectable.[6]. We now consider the imaging of both coherent and incoherent fields.

The field in the focal plane is given in the Kirchoff approximation by[7,8]

$$p(\rho, f) = \frac{k}{2\pi i}\int_S d^2\rho' \frac{e^{ikr}}{r} L(\rho') p(\rho', 0) \tag{1}$$

where $L(\boldsymbol{\rho}')$ is the effect of the focusing device which in the optical case would be a lense. The relation between r, $\boldsymbol{\rho}'$, $\boldsymbol{\rho}$ and f is shown in Fig. 5.

For $f >> \rho, \rho'$ we obtain

$$\begin{aligned} r &= \sqrt{f^2 + |\boldsymbol{\rho} - \boldsymbol{\rho}'|^2} \\ &\cong f + \left(\rho^2 - 2\boldsymbol{\rho} \bullet \boldsymbol{\rho}' + \rho'^2\right)/2f \end{aligned} \tag{2}$$

The term involving ρ'^2 is usually referred to as the Fresnel correction. Employing the customary procedure of retaining all terms of (2) in the phase in (1) but setting $r = f$ in the amplitude, which is less sensitive to small corrections, we have

$$p(\boldsymbol{\rho}, f) \cong \frac{k}{2\pi i} \frac{e^{ikf + ik\rho^2/2f}}{f} \int_S d^2\boldsymbol{\rho}' \, e^{-ik\boldsymbol{\rho}\bullet\boldsymbol{\rho}'/f + ik\rho'^2/2f} L(\boldsymbol{\rho}') p(\boldsymbol{\rho}', 0) \tag{3}$$

If only the first term in the phase of the integrand were now retained, we would have the far field (Fraunhoffer) approximation while if the second term in the phase of the integrand is retained we have the Fresnel approximation. The effect of the lense is to cancel out this second term and yield the Fraunhoffer image in the focal plane [9]. We thus set[10]

$$L(\boldsymbol{\rho}') = e^{-ik\rho'^2/2f} \tag{4}$$

and obtain

$$p(\boldsymbol{\rho}, f) \cong \frac{k}{2\pi i f} e^{ik(f + \rho^2/2f)} \int_S d^2\boldsymbol{\rho}' e^{-ik\boldsymbol{\rho}\bullet\boldsymbol{\rho}'/f} p(\boldsymbol{\rho}', 0) \tag{5}$$

The field in the focal plane, $p(\boldsymbol{\rho},f)$, has now been expressed as an integral over the field in the plane of the receiver $p(\boldsymbol{\rho},0)$.

The field in the receiver plane, $p(\boldsymbol{\rho},0)$, may be considered to be composed of a coherent part that represents the information of interest and a random part that is due to scattering by inhomogeneities in the medium. As in Section B, we treat the randomness of the pressure wave by calculating $|p(\boldsymbol{\rho},f)|^2$, a quantity proportional to the intensity of the wave, and then introduce a correlation function to describe the fluctuations that are now associated with the sound field at the receiver rather than with fluctuations in the properties of the medium.

From (5) we have

$$\left\langle |p(\boldsymbol{\rho}, f)|^2 \right\rangle = \left| \frac{k}{2\pi i f} \right|^2 \int_S d^2\boldsymbol{\rho}' \int_S d^2\boldsymbol{\rho}'' e^{-ik\boldsymbol{\rho}\bullet(\boldsymbol{\rho}'-\boldsymbol{\rho}'')/f} \mu(|\boldsymbol{\rho}' - \boldsymbol{\rho}''|) \tag{6}$$

where, following the procedure used in part B, we have set

$$\mu(|\boldsymbol{\rho}' - \boldsymbol{\rho}''|) = \left\langle p^*(\boldsymbol{\rho}', 0) p(\boldsymbol{\rho}'', 0) \right\rangle \tag{7}$$

As noted in Section B, this choice for a correlation function implies an assumption that the fluctuating quantity, here the sound field, is both homogeneous and isotropic.

The coherent field. The above result is immediately specialized to the case of a coherent field by setting $\mu(|\boldsymbol{\rho}'-\boldsymbol{\rho}''|) = p_0^2$ where p_0^2 is proportional to the intensity of the incident wave. In this limit there is no coupling between $\boldsymbol{\rho}'$ and $\boldsymbol{\rho}''$ and we have

$$\begin{aligned} \frac{\left\langle |p_{coh}(\boldsymbol{\rho}, f)|^2 \right\rangle}{(p_0 kA/2\pi f)^2} &= \frac{1}{A^2} \left| \int_S d^2\boldsymbol{\rho}' e^{-ik\boldsymbol{\rho}\bullet\boldsymbol{\rho}'/f} \right|^2 , \quad A = \text{Area of Receiver} \\ &= \left[\frac{J_1(k\rho a/f)}{k\rho a/2f} \right]^2 , \quad \text{circular receiver, } A = \pi a^2 \\ &= \left[\frac{\sin(kxh/2f)}{kxh/2f} \right]^2 \left[\frac{\sin(kyh/2f)}{kyh/2f} \right]^2 , \quad \text{square receiver, } A = h^2 \end{aligned} \tag{8}$$

where J_1 refers to the Bessel function of first order. Both of these expressions have a form that peaks at unity at the center of the receiver. The results for the two geometries are compared in Fig. 6 in which $\langle |p_{coh}|^2 \rangle / p_C^2$, with $p_C \equiv p_0 kA/2\pi f$, is plotted as a function of distance from the center for both a circular and a square receiver. The square case is considered because, as summarized below, it is possible to obtain a simple complete description of the incoherent field for this geometry(11).

For the circular receiver, we first set $k = 2\pi/\lambda$ and write the argument of the Bessel function as

$$\frac{k\rho a}{f} = 2\pi \frac{a}{\lambda} \frac{a}{f} \frac{\rho}{a} \tag{9}$$

The choices $\lambda = 0.3$ meter (which follows from a sound velocity of 300 meters/sec. and a frequency of 1000 Hz.) as well as $a = 0.5$ meter and $f = 1$ meter, have been used. The result is given by the curve marked "1" in Fig. 6.

For the square receiver we consider distance from the center along a diagonal $x = y$ indicated by curve "2" in Fig. 6, as well as along a coordinate line ($y = 0$, $0 < x < h/2$). The latter curve is indicated by "3" in Fig. 6. (Since on the diagonal a radial distance R from the center corresponds to a value of x equal to $R \cos \pi/4 = R/\sqrt{2}$, for the graph marked "2" x has been replaced by $x/\sqrt{2}$ to account for this scaling.) As expected, near the center curves 2 and 3 yield equal values for the coherent field intensity. The correspondence between circular and square receivers is also found to be quite close as should also be expected. For numerical values in the rectangular case we have used $h/2 = 0.5$ meter with the other parameters remaining the same as for the circular case.

Incoherent field. Here we must make a choice for the correlation function. As noted above, the choice is a balance between physical realism and analytical tractability and the Gaussian is frequently chosen. We adopt this form here and set

$$\mu(|\boldsymbol{\rho}' - \boldsymbol{\rho}''|) = p_F^2 e^{-|\rho' - \rho''|^2 / L^2} \tag{10}$$

where p_F^2 is proportional to the mean square intensity of the fluctuating field and L is the correlation length, i.e. the distance over which the fluctuations in the field display some coherence. We are thus introducing a new length into the considerations and can examine results as a function of the ratio of the receiver size, a or h, to the correlation length L. For arbitrary ratios of receiver size to correlation length it is found that the results can be obtained in a simple, readily interpretable form only for the rectangular receiver. For the circular case it appears that only the large receiver limit $a/L \rightarrow \infty$ can be treated in this manner(12). The results are of considerable interest since they show that the fluctuations in the image are diminished by increasing the receiver size until it is about twice the correlation length L. This result is analogous to the optical effect that the twinkling of stars appears greater to the naked eye than to a larger optical receiver.

For the square case we write

$$\boldsymbol{\rho} \bullet (\boldsymbol{\rho}' - \boldsymbol{\rho}'') = x(x' - x'') + y(y' - y'') \tag{11}$$

and express (6) in the form

$$\left\langle \left| p_{incoh}(\boldsymbol{\rho}, f) \right|^2 \right\rangle = p_F^2 \left(\frac{kh^2}{2\pi f} \right)^2 M(h / L, \gamma_x) M(h / L, \gamma_y) \tag{12}$$

where

$$M(h/L,\gamma_x) \equiv \frac{1}{h^2}\int_{-h/2}^{h/2} dx' \int_{-h/2}^{h/2} dx'' e^{-ikx(x'-x'')/f-(x'-x'')^2/L^2} \tag{13}$$

and $2\gamma_x$ = kxL/f. The factor $M(h/L,\gamma_y)$ has the same form as $M(h/L,\gamma_x)$ except that x is replaced by y . These quantities have been defined so that they reduce to unity at the center of a very large receiver, i.e., $M(\infty,0) = 1$. (It should be noted that results for a rectangular receiver may be obtained by merely modifying the limits on the integral for either $M(h/L,\gamma_x)$ or $M(h/L,\gamma_y)$.

The details of the integration are summarized in Appendix A. One obtains

$$M(h/L,\gamma_x) = 2\left(\tfrac{L}{h}\right)^2\left(\tfrac{h}{L}P - Q\right) \tag{14}$$

where

$$\begin{aligned} P &= \tfrac{1}{2}\sqrt{\pi}e^{-\gamma_x^2}\,\mathrm{Re}\{F(h/L,\gamma_x)\} \\ Q &= \tfrac{1}{2}\left[1 - e^{-(h/L)^2}\cos(2\gamma_x h/L)\right] + \tfrac{1}{2}\sqrt{\pi}e^{-\gamma_x^2}\,\mathrm{Im}\{F(h/L,\gamma_x)\} \end{aligned} \tag{15}$$

in which

$$F(h/L,\gamma_x) \equiv erf\left(\tfrac{h}{L} + i\gamma_x\right) - erf(i\gamma_x) \tag{16}$$

and

$$erf(z) = \tfrac{2}{\sqrt{\pi}}\int_0^z dte^{-t^2} \tag{17}$$

Results of the same form occur for the y dependence with γ_y = kyL/2f being used in place of γ_x.

To obtain some understanding of this result, we now examine various special cases. It is convenient to use the coefficient in (12) as a reference value and set

$$p_R^2 \equiv \left(\frac{p_F k h^2}{2\pi f} \right)^2 \tag{18}$$

so that

$$\frac{\left\langle \left| p_{incoh}(\rho, f) \right|^2 \right\rangle}{p_R^2} = M(h/L, \gamma_x) M(h/L, \gamma_y) \tag{19}$$

1) Field at the center of the receiver $(x = y = 0)$ as a function of h/L In this case, $\gamma_x = \gamma_y = 0$ and from (19) we have

$$\frac{\left\langle \left| p_{incoh}(0, f) \right|^2 \right\rangle}{p_R^2} = [M(h/L, 0)]^2 \tag{20}$$

The results in (14) to (16) yield

$$M(h/L, 0) = \sqrt{\pi} \left(\frac{L}{h} \right)^2 \left[\frac{h}{L} erf\left(\frac{h}{L} \right) + \frac{e^{-(h/L)^2} - 1}{\sqrt{\pi}} \right] \tag{21}$$

as obtained by Chernov(13). A graph of (20) is shown as the solid curve in Fig. 7. A graph of $\exp[-(h/L)^2]$ has been included for comparison. The fluctuations are seen to attain their maximum value in the limit of small receiver size to correlation length $(h/L << 1)$ and to decrease rapidly as h/L increases until a ratio of h/L equal to about two is obtained, after which they decrease more slowly. As noted above, this decrease in the effect of fluctuations is well known in astronomical observations where the scintillation of stars is found to be much larger to the naked eye than when observed with large optical receivers.

2) Noncentral points To examine the corresponding situation at various non central receiver locations, we write $p_{incoh}(\rho, f) = p_{incoh}(x, y, f)$ and consider, in Fig. 8, the value of $< |p_{incoh}(x,x,f)|^2 > / p_R^2$, i.e. the field at locations along the diagonal $x = y$, for $x = 0.1h$, $0.3h$ and $0.5h$.

In obtaining these results we have had to make a choice for the parameters involved in the definition of $2\gamma_x = kxL/f$. Setting $k = 2\pi/\lambda$, we first write

$$2\gamma_x = 2\pi \frac{L}{\lambda} \frac{L}{f} \frac{x}{h} \frac{h}{L} \tag{22}$$

The choices $\lambda = .3$ meters and $f = 0.2$ meters have again been used as well as L= 0.1 meter. No attempt at a thorough parameter study has been made at this stage. Although the result in Fig. 8 predicts a more rapid decrease in the fluctuations as one moves away from the center, there is probably no advantage to be gained from this decrease since the coherent field itself falls off as one moves away from the center (cf. Fig. 6).

3) Spatial Dependence for fixed h/L We first consider the case of large receiver to correlation length ratio (h/L >> 1). This limit is easily treated by merely setting h/L = ∞ in the upper limit of the integrals that define P and Q as given in Appendix A. We then obtain

$$M(h/L,\gamma) \approx \frac{\sqrt{\pi}L}{h} e^{-\gamma^2} , \qquad h/L >> \gamma \left(= \gamma_x, \gamma_y\right) \tag{23}$$

and find

$$\frac{\left\langle \left| p_{incoh}(x,y,f) \right|^2 \right\rangle}{p_R^2} = \frac{\pi L^2}{h^2} e^{-(kL/f)^2 (x^2+y^2)} \tag{24}$$

This result has the same functional form as that given by Ishimaru[14] for the large circular receiver with $x^2 + y^2 = r^2$. As noted by Chernov[13], far from the edge of the receiver, where shape effects should be negligible, results for both square and circular receivers can be expected to be quite similar.

For h/L = 1, 2 and 4 and field points on the diagonal (i.e., y = x), we obtain the results shown in Fig. 9. The decrease in the magnitude of p_{incoh} associated with increasing values of h/L is consistent with the earlier results for dependence of fluctuations on receiver size shown in Fig. 7.

Appendix A Evaluation of $M(h/L,\gamma_x)$

From (12) of Section C we have

$$M(h/L,\gamma_x) \equiv \frac{1}{h^2}\int_{-h/2}^{h/2} dx' \int_{-h/2}^{h/2} dx'' e^{-ikx(x'-x'')/f-(x'-x'')^2/L^2} \tag{A.1}$$

Consider this integral as being taken over a square of area h^2 in an x'-x" plane. Separating variables in the integrand by introducing u = (x' – x") and v = (x' + x")/2, a transformation for which dx'dx" = dudv, we integrate over the same area in the u-v plane by evaluating

$$h^2 M(h/L,\gamma_x) = \int_{-h}^{0} du \int_{-(h+u)/2}^{(h+u)/2} dv e^{-i(kx/f)u-(u/L)^2} + \int_{0}^{h} du \int_{-(h-u)/2}^{(h-u)/2} dv e^{-i(kx/f)u-(u/L)^2} \tag{A.2}$$

The area is shown in Fig. 10 where two examples of the area strips that are summed in this integration process are indicated. When the v integration is carried out we find

$$M(h/L,\gamma_x) = 2\left(\tfrac{L}{h}\right)^2 \left(\tfrac{h}{L}P - Q\right) \tag{A.3}$$

where

$$P = \int_0^{h/L} d\xi e^{-\xi^2} \cos 2\gamma\xi = \mathrm{Re}\left\{\int_0^{h/L} d\xi e^{-\xi^2} e^{2i\gamma\xi}\right\}$$
$$Q = \int_0^{h/L} d\xi e^{-\xi^2} \xi \cos 2\gamma\xi = \mathrm{Re}\left\{\int_0^{h/L} d\xi e^{-\xi^2} \xi e^{2i\gamma\xi}\right\} \tag{A.4}$$

with ξ = u/L and 2γ = kxL/f. These integrals may be expressed in terms of the complex error function. The results are given in (14) - (17).

For h/L >> 1, we replace the upper limit on each integral in (A.4) by ∞ and have

$$P = \int_0^{\infty} d\xi e^{-\xi^2} \cos 2\gamma\xi = \tfrac{1}{2}\sqrt{\pi} e^{-\gamma^2}$$
$$Q = \int_0^{\infty} d\xi e^{-\xi^2} \xi \cos 2\gamma\xi = \int_0^{\infty} d\xi e^{-\xi^2} \xi \left[1 - \tfrac{(2\gamma\xi)^2}{2!} + \ldots\right] \approx \frac{1}{2} - \gamma^2 + \ldots \tag{A.5}$$

Since P is multiplied by h/L in (A.3), the contribution from Q is negligible unless γ >>1.

References

1. L. Amundsen, B. Arntsen and R. Mittet, "Depth Imaging of Offset Vertical Seismic Profile Data," Geophysical Prospecting, **41**, 1009-1031, (1993).

2. If spatial variations in the density, rather than the bulk modulus, were considered, we would obtain the more complicated wave equation

$$\frac{\partial^2 P}{\partial t^2} - (B/\rho)\nabla^2 P + (B/\rho)\nabla(\ln \rho) \bullet \nabla P = 0$$

At this preliminary stage in the analysis where only a qualitative understanding of the problem is being developed, it seems appropriate that this more complicated wave equation, along with the shear wave considerations, should be neglected.

3. A. Erdelyi, ed. *Tables of Integral Transforms,* McGraw Hill, New York, (1954), Vol. 2, p. 29, No. 10.

4. Ref. 3, Vol. 1, p. 73, No. 19.

5. Ref. 3, Vol. 1, p. 152, No. 14 and p. 89, No. 12.

6. A. Ishimaru, *Wave Propagation in Random Media*, Academic Press, New York (1978), Vol. 2, p. 305.

7. Ref. 6, p. 302.

8. M. Born and E. Wolf, *Principles of Optics*, 3rd. (Revised) Ed., Pergamon Press (1965), New York, pp. 382 - 385.

9. Ref.8, pp. 384 - 385.

10. Ref. 6, p. 302.

11. L. A. Chernov, *Wave Propagation in a Random Medium*, Dover (1960), New York, p. 137.

12. Ref. 6, p.304.

13. Ref.1, p.153.

14. Ref. 6, p. 304.

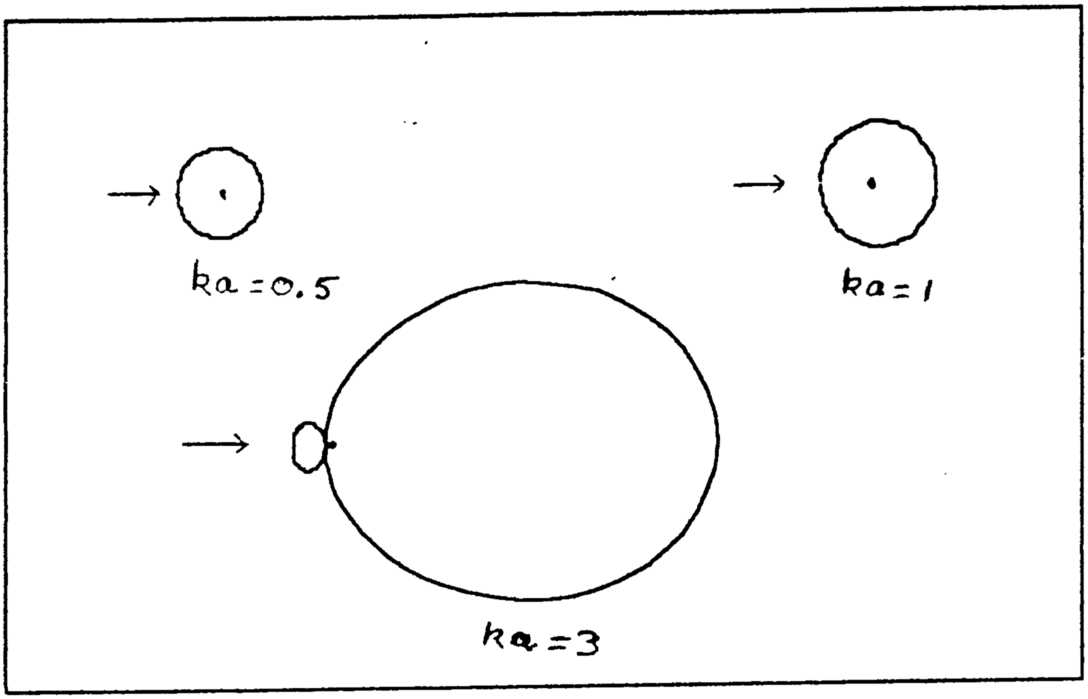

Fig. 1

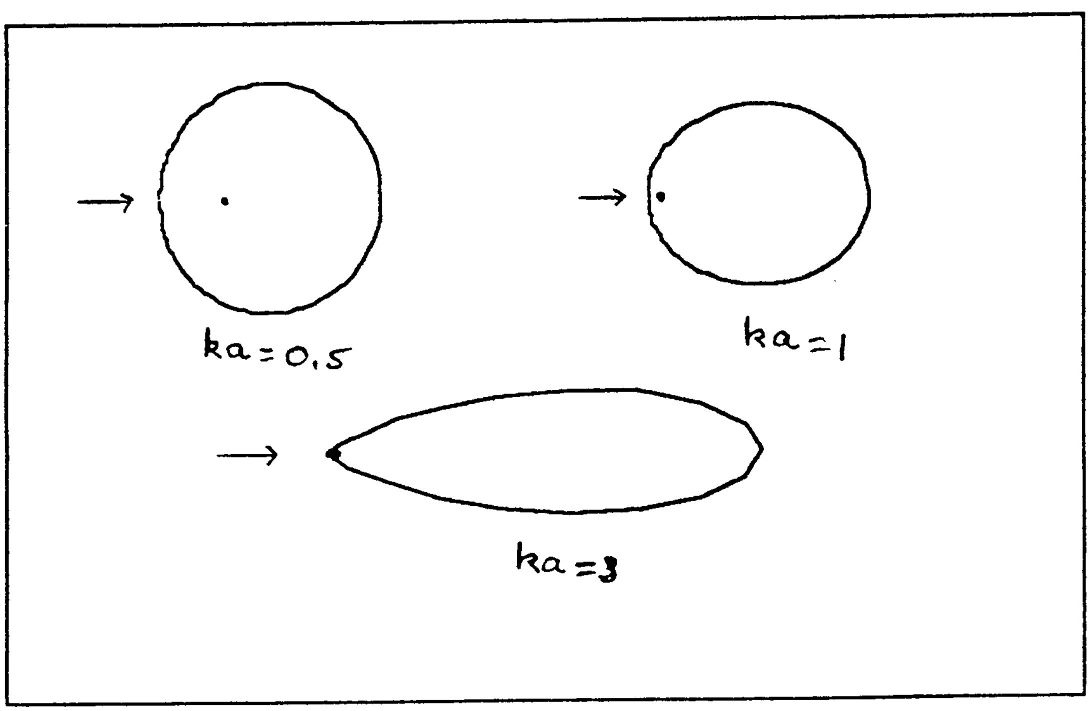

Fig. 2

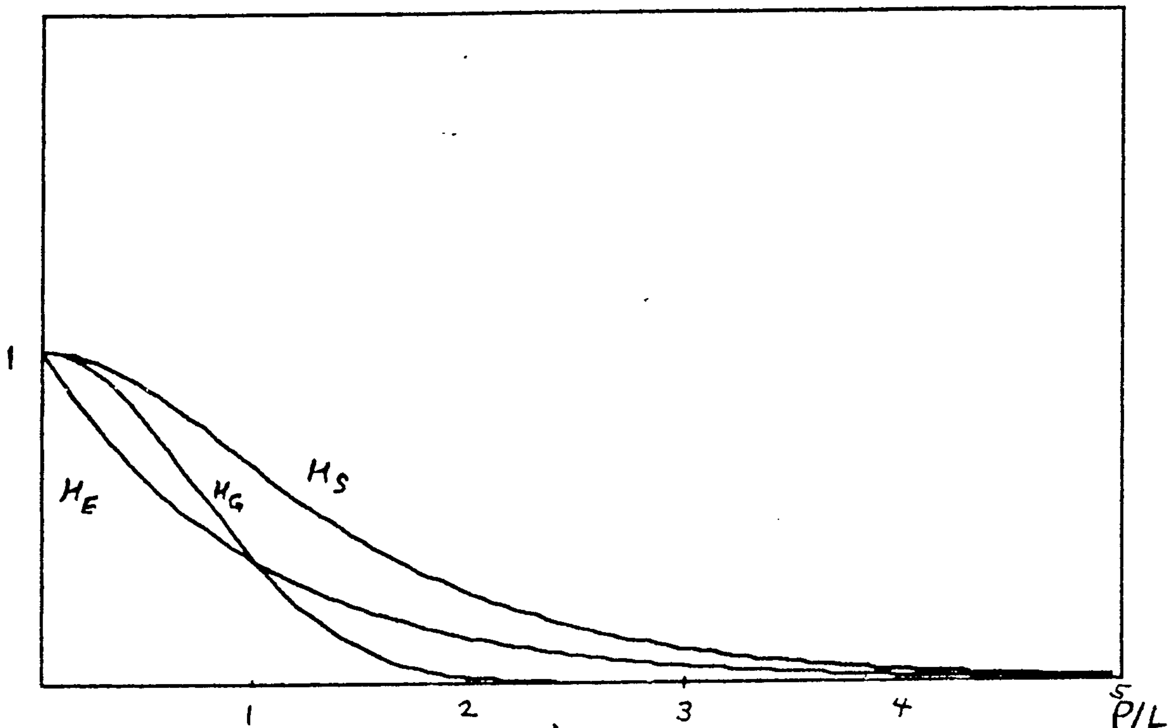

Fig. 3

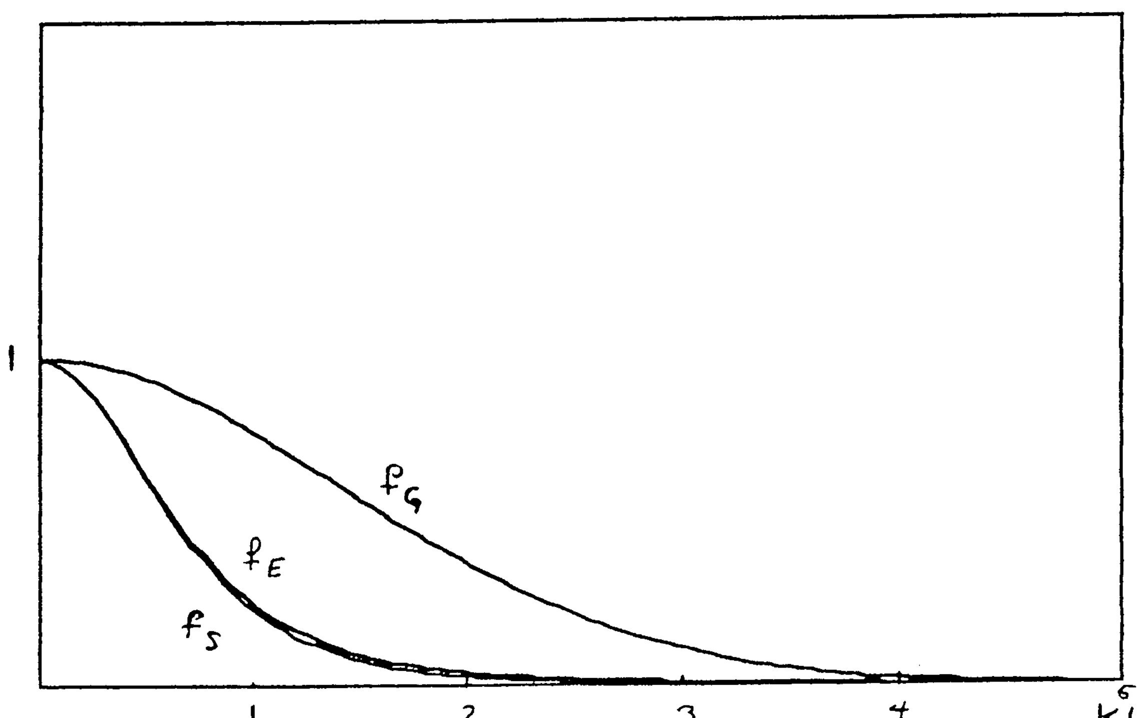

Fig. 4

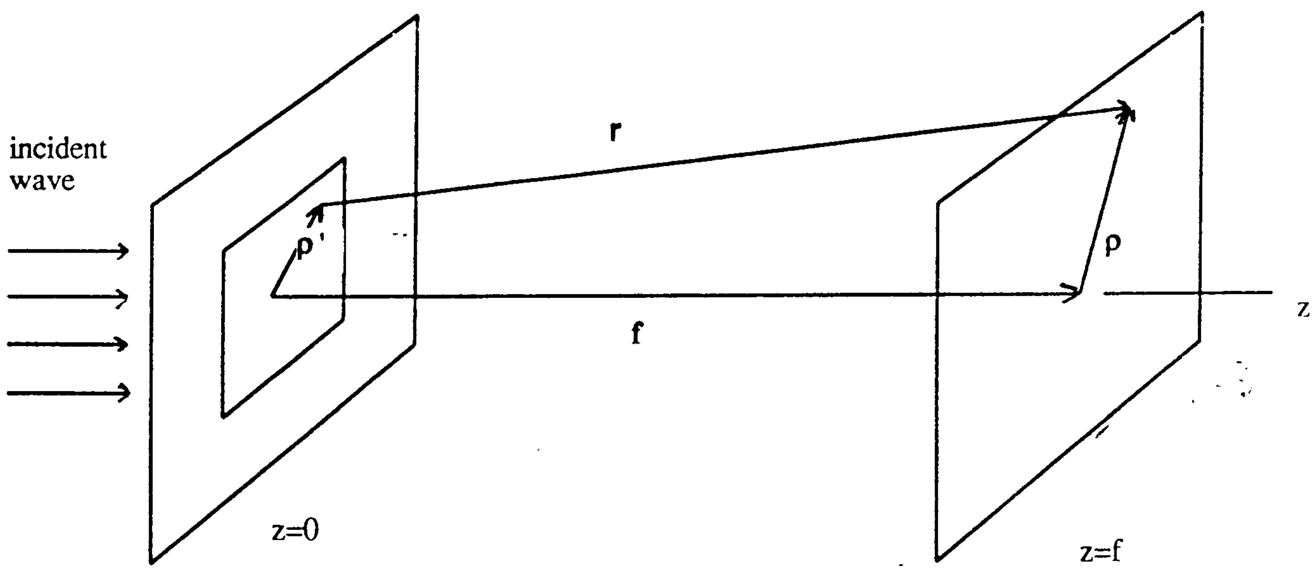

Fig. 5

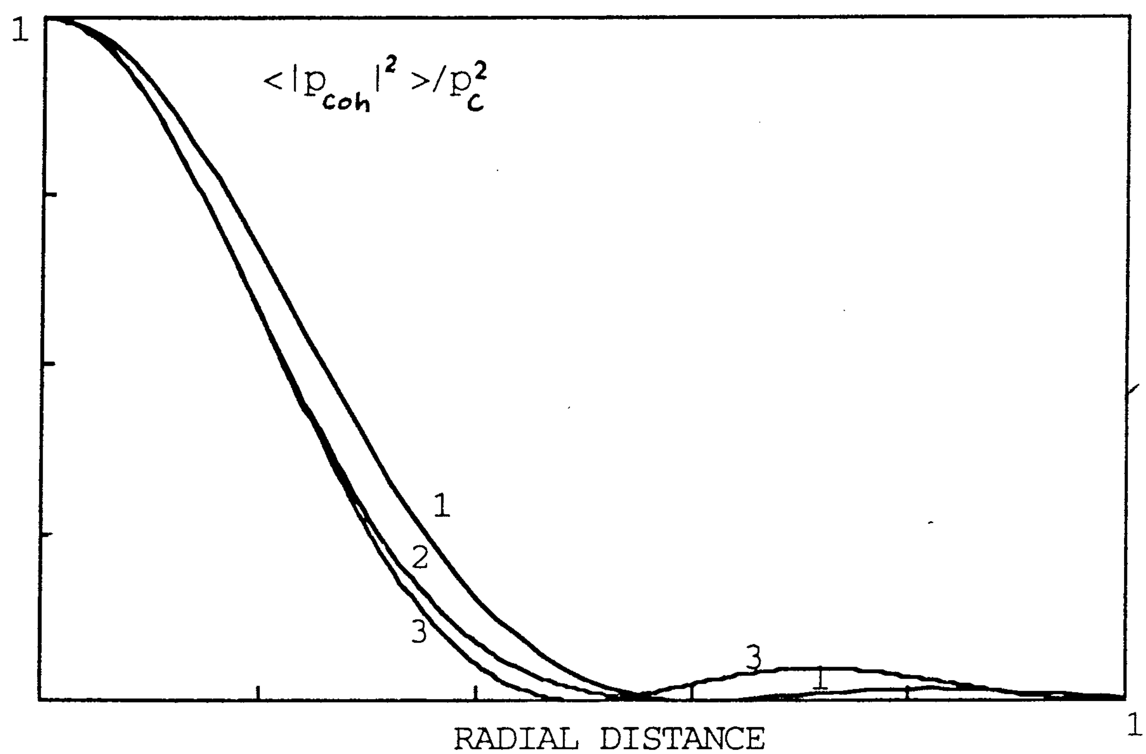

Fig. 6

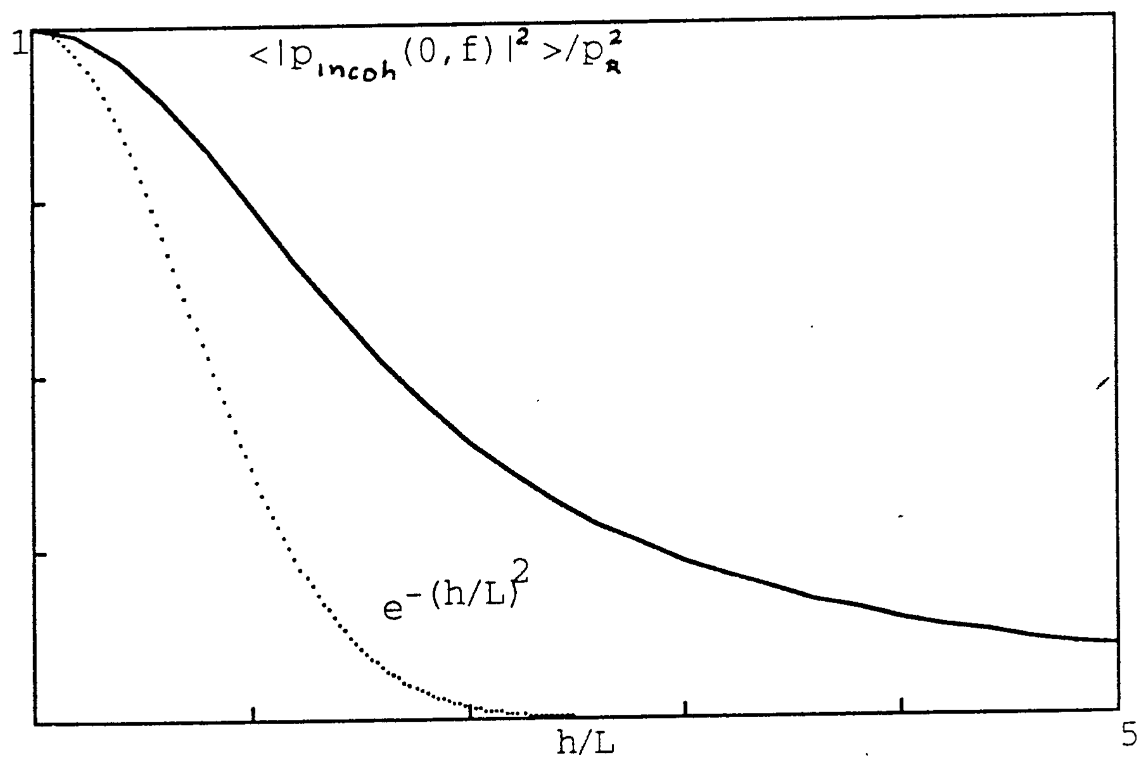

Fig. 7

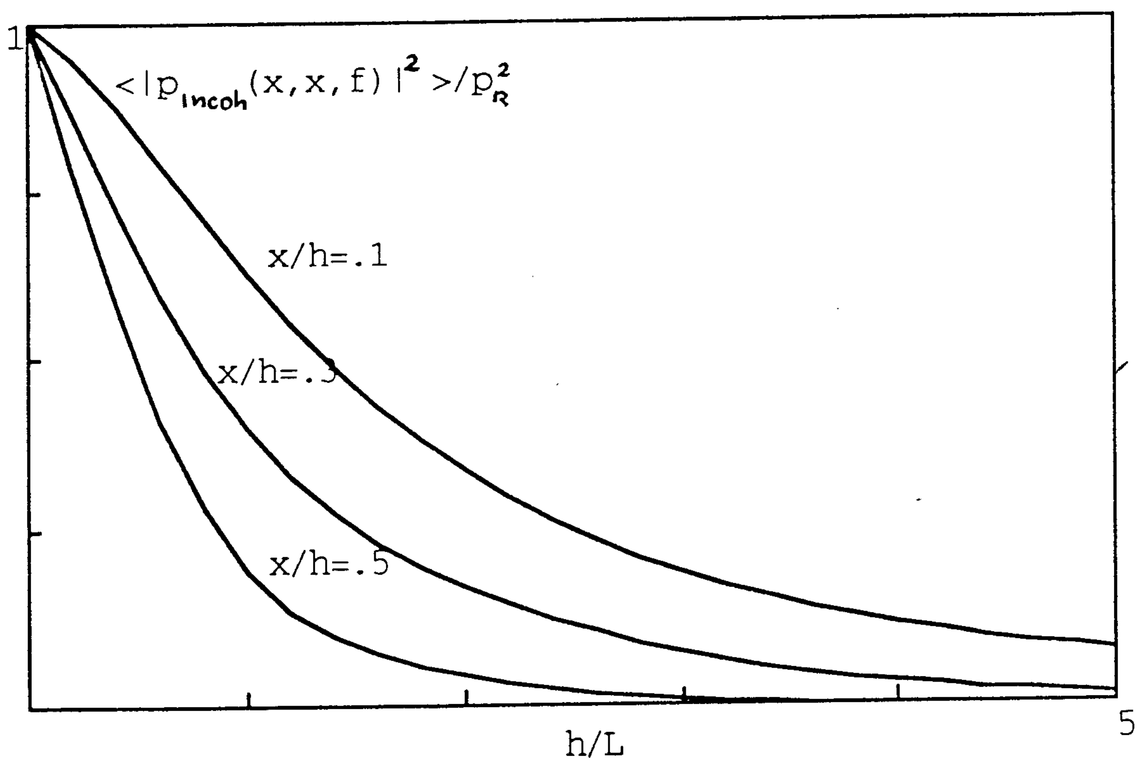

Fig. 8

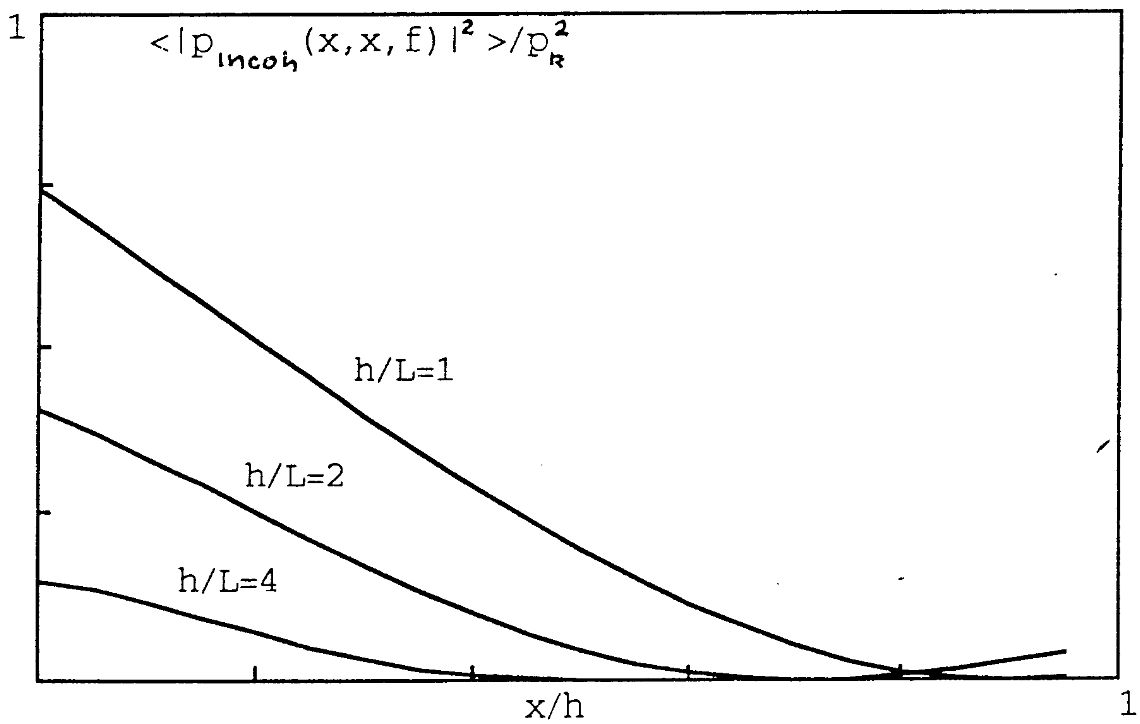

Fig. 9

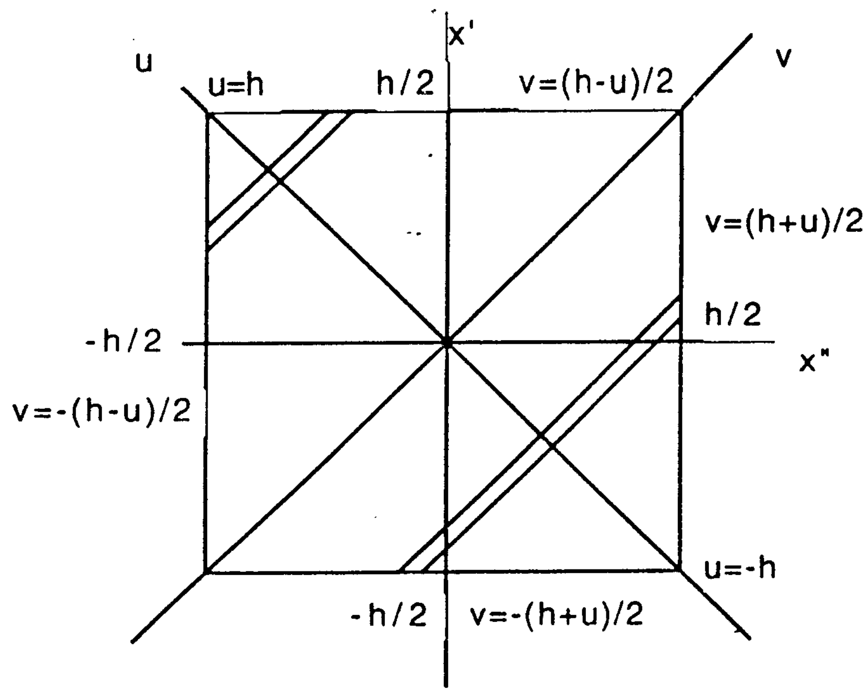

Fig. 10